Tandem Repeats of a Specific Alternating Purine–Pyrimidine DNA Sequence Adjacent to Protamine Genes in the Rainbow Trout That Can Exist in the Z Form†

Judd M. Aiken,‡ Freda D. Miller, Fred Hagen, Debbie I. McKenzie, Stephen A. Krawetz, Johan H. van de Sande, J. B. Rattner, and Gordon H. Dixon*

Department of Medical Biochemistry, Faculty of Medicine, The University of Calgary, Calgary, Alberta, Canada T2N 4N1

Received February 14, 1985

ABSTRACT: We have located an extensive $(AC)_n$-rich but specific sequence downstream of three rainbow trout protamine genes. Although sharing considerable sequence homology, including a perfectly conserved 46 base pair repeat, the sequences exhibit a regular heterogeneity in the length of the $(AC)_n$-rich tracts. Radioimmunoassay experiments, S1 nuclease sensitivity studies, two-dimensional electrophoretic analysis, and immunoelectron microscopy studies have been used to determine if the region could assume a Z DNA conformation. It was found that, in a supercoiled plasmid, the $(AC)_n$-rich region has the ability to attain the Z DNA conformation under physiological conditions.

An increasing body of evidence points to the existence of potential Z DNA regions in the eukaryotic genome. Antibodies specific to the Z DNA conformation have been used to detect and map the presence of the left-handed conformation in fixed (Nordheim et al., 1981; Jovin et al., 1982) and unfixed (Arndt-Jovin et al., 1983) dipteran polytene chromosomes, protozoan micronuclei (Robert-Nicoud et al., 1984), PM2 DNA (Miller et al., 1983), SV40 minichromosomes (Nordheim & Rich, 1983), and a number of rat tissues (Morgenegg et al., 1983).

Z DNA has been implicated in the regulation of eukaryotic genomes. The transcriptionally active micronucleus but not the inactive micronucleus of ciliated protozoans has been found to exhibit immunoreactivity to Z-specific antibodies (Lipps et al., 1983; Robert-Nicoud et al., 1984). SV40 viral transcriptional enhancer sequences were found to contain three Z DNA antibody binding sites located within and adjacent to the 72 base pair (bp) repeat (Nordheim & Rich 1983).

Hamada et al. (1982) reported that AC alternating sequences are highly conserved throughout eukaryotic genomes while GC-rich sequences are not ubiquitous. Small blocks of AC repeats have been reported for a human globin gene (Miesfeld et al., 1981), a mouse immunoglobin gene (Nichioka & Leder, 1980), human actin gene (Hamada et al., 1982; Hamada & Kakunaga, 1982), and an Alu family sequence (Saffar & Lerman, 1983).

A 146 base pair $(AC)_n$-rich region, containing two perfect 46 base pair repeats, has been detected downstream of a trout protamine gene (Aiken et al., 1983). Two similar regions in different protamine clones have now been sequenced and found to contain identical 46 base pair sequences: in one case a single repeat, and in the second, three repeats. Since Z DNA has been implicated in the control of transcription (Nordheim & Rich, 1983), we have investigated the ability of one of the $(AC)_n$-rich regions to attain the Z DNA conformation under physiological conditions. Radioimmunoassay studies using Z DNA specific antibodies have been coupled with electron microscopic localization of Z DNA antibody binding sites as well as S1 nuclease sensitivity and two-dimensional gel electrophoresis studies to determine (a) if the $(AC)_n$-rich region can assume a left-handed conformation in vitro and (b) the conditions required to promote a B to Z conformational shift. We report that this region, in a supercoiled plasmid, can assume a Z DNA conformation under physiological conditions and that other alternating purine–pyrimidine regions close to the $(AC)_n$-rich sequence also react with the Z DNA specific antibody.

Experimental Procedures

Recombinant DNA and DNA Sequence Analysis. The isolation of the protamine clones from a Charon 4A *Eco*RI trout library has been previously described (Aiken et al., 1983). DNA sequence analysis employed the chemical degradation method of Maxam & Gilbert (1980).

Anti-Z DNA IgG. The T4 polyclonal anti-Z DNA immunoglobulin G (IgG) was a gift of Dr. D. Zarling (Zarling et al., 1984). ^{32}P-Labeled poly[d(Gm^{5}C)] was synthesized by a modification of the procedure of Gil et al. (1974) in a reaction containing 3 mM dGTP and 3 mM d[m^{5}CTP] (P-L Biochemicals) in the presence of [α-^{32}P]dGTP (New England Nuclear).

Competitive Radioimmunoassay. Formation of the antibody–DNA complex was monitored by competition between unlabeled plasmid DNA and ^{32}P-labeled poly[d(Gm^{5}C)] for anti-Z IgG in either high-salt [4.0 M NaCl, 40 mM tris(hydroxymethyl)aminomethane hydrochloride (Tris-HCl), pH 7.2, 4.0 mM ethylenediaminetetraacetic acid (EDTA)] or low-salt buffer (0.12 M NaCl, 4.0 mM $MgCl_2$, 40 mM Tris-HCl, pH 7.2). The ^{32}P-labeled poly[d(Gm^{5}C)] probe was incubated at 65 °C for 30 min and centrifuged for 15 min at 9000*g*, and the supernatant (which contained 6 ng of DNA) was used in the subsequent assay. Various dilutions of plasmid DNA (20 μL) were added to 10 μL of labeled probe in a final volume of 110 μL and equilibrated for 30 min at 65 or 37 °C in high- or low-salt buffer, respectively. Anti-Z IgG was added, and the reaction mixtures were incubated for 1 h at 54 (high-salt buffer) or 37 °C (low-salt buffer). Goat anti-rabbit IgG (Miles-Yeda) was subsequently added as a second antibody carrier. After incubation for 1 h at room temperature, 1 mL of the appropriate high- or low-salt buffer was added, and the reactions were centrifuged for 15 min at 9000*g*. The immunoprecipitates were washed once more with high-salt or low-

† This work was supported by a W. H. Davies Fellowship to J.M.A., a Medical Research Council Studentship to F.D.M., an Alberta Heritage Foundation for Medical Research Studentship to D.I.M., and Medical Research Council of Canada grants to J.H.v.d.S. and G.H.D. J.B.R. is an Alberta Heritage Foundation for Medical Research Scholar.

‡ Present address: Department of Anatomy, Physiology and Radiology, North Carolina State University School of Veterinary Medicine, Raleigh, NC 27606.

0006-2960/85/0424-6268$01.50/0

salt buffer prior to resuspension in 0.1 N NaOH. Samples were counted in 10 mL of Aquasol 2 (New England Nuclear) neutralized with Tris-HCl.

Electron Microscopy. Samples for electron microscopy were prepared by incubating 3.8–5.0 μg of plasmid DNA in 40–50 μL of high-salt buffer (3.8 M NaCl, 38 mM Tris-HCl, 3.8 mM EDTA, pH 7.8) or low-salt buffer (100 mM NaCl, 38 mM Tris-HCl, 3.8 EDTA, pH 7.8) for 1 h at 37 °C. The T4 anti-Z IgG was added to the DNA–buffer solution at an antibody:TP17 molar ratio of either 95:1 or 379:1, and the reactions were incubated for 1 h at 55 °C (high and low salt). Subsequently, 3 μL of ferritin-conjugated purified goat anti-rabbit IgG (Miles-Yeda; 1:100 dilution of 15 mg/mL) was added and incubated at 37 °C for 1 h. The samples were sequentially fixed in 1% formaldehyde and 0.6% glutaraldehyde at 4 °C for 15 min. Samples were dialyzed overnight against 10 mM Tris-HCl, pH 7.6, and 0.1 mM NaCl, prior to cleavage with *Kpn*I, and prepared for electron microscopy as described by Stockton et al. (1983). Electron micrographs were analyzed by using a Microplan II image analysis system.

S1 Nuclease Reactions. DNA samples were incubated with 5–50 units of S1 (Bethesda Research Laboratories) per microgram of DNA in 3 mM sodium acetate, 120 mM sodium chloride, and 0.3 mM zinc chloride (pH 4.5) at 37 °C for 30 min. The samples were then phenol extracted and ethanol precipitated prior to digestion with *Msp*I (4 units per microgram) for 1 h.

Southern Hybridization Analysis. The S1 and restriction endonuclease digestion products were fractionated on a 1.5% agarose gel and transferred to nitrocellulose in 10 × standard saline citrate (SSC). Hybridizations were performed for 12 h at 42 °C in 4 × SET (0.15 M NaCl, 1 mM EDTA, 20 mM Tris-HCl, pH 7.8), 50% formamide, 10 × Denhardt's solution, 0.1% sodium dodecyl sulfate (SDS), and 100 μg/mL yeast RNA. The transfer was washed at 55 °C in 1 × SSC and 0.1% SDS. The $(AC)_n$ probe was labeled by nick translation (Maniatis et al., 1982) using [α-^{32}P]dATP (Amersham).

Two-Dimensional Gel Electrophoresis To Resolve Plasmid Topoisomers. Topoisomers of pRSA containing the $(AC)_n$ repeat excised by *Rsa*I and the control pUC9 for gel electrophoresis (Viera & Messing, 1982) were prepared in vitro by relaxation of form I plasmid DNA with calf thymus topoisomerase in the presence of 0–10.0 μM ethidium bromide (Lee & Morgan, 1978). The relaxed samples were then extracted 3 times with equal volumes of buffer-saturated phenol and once with phenol–chloroform. The topoisomer mixtures thus prepared were separated on a 0.7% agarose gel in Tris–borate–EDTA (TBE) buffer (Wang et al. 1982) to ensure an adequate distribution of topoisomers. The separate topoisomer populations were mixed for two-dimensional gel electrophoretic analyses. Control samples were prepared with and without the addition of ethidium bromide and/or topoisomerase.

Two-dimensional electrophoretic analysis was performed on agarose gels ranging from 0.8% to 1.5% in TBE buffer. The mixed topoisomers were applied to the gels and electrophoresed in the first dimension at 4 V/cm for 6–18 h. The gels were subsequently incubated in buffer containing 0.5–1.3 μg/mL chloroquine for 8 h and electrophoresed in the second dimension in buffer containing the same concentration of chloroquine. The gels were incubated in 0.1 × TBE for 1 h prior to staining in 0.5 μg/mL ethidium bromide and then destained and photographed.

Computer-Assisted Data Analysis. Query sequences were searched against the GenBank data base, and similar sequences were aligned with the use of the Beckman MicroGenie Make

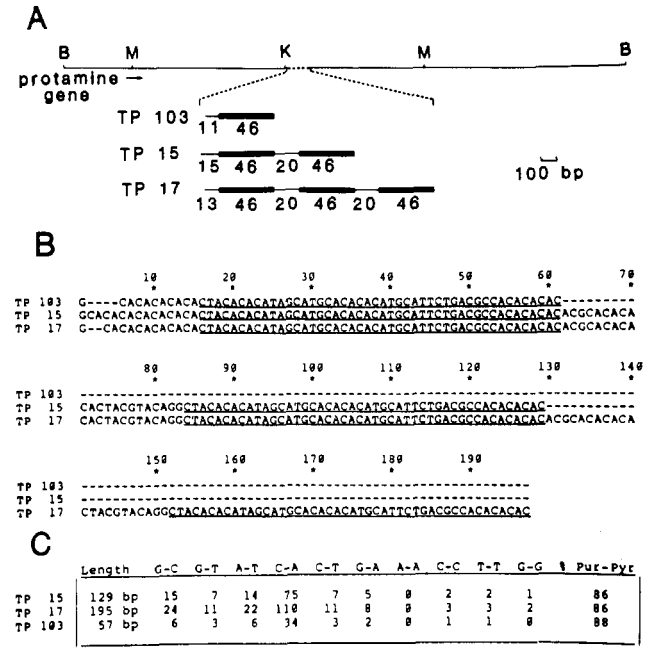

FIGURE 1: (A) Proximity of the $(AC)_n$-rich sequences to the protamine genes in clones TP103, TP15, and TP17. The $(AC)_n$-rich sequences are schematically represented with solid bars indicating the 46 base pair repeat common to all three clones. *Bam*HI (B), *Msp*I (M), and *Kpn*I (K) restriction endonuclease sites are indicated. (B) Comparison of the nucleotide sequences of the $(AC)_n$-rich regions between clones TP103, TP15, and TP17. The 46 base pair repeat region is underlined. Base 1 is 10 nucleotides downstream of the *Kpn*I site in panel A. Dashes have been inserted to indicate gaps, introduced for optimal sequence alignment. (C) Dinucleotide pair combinations present in the $(AC)_n$-rich sequences of TP15, TP17, and TP103.

Search program (see paragraph at end of paper regarding supplementary material). In any repeating sequence of the type $(AC)_n$ or $(TG)_n$, there will be many overlapping alignments; the ones depicted in Table I are those achieving the maximum identity score. The identity score (maximum overall identity) was defined as the number of bases matched times the percent of identical bases. Relative homology between the $(AC)_n$ or $(TG)_n$ sequences and those identified in the data base was defined as the identity score divided by the maximum possible identity score.

RESULTS

Sequence and Organization of $(AC)_n$-Rich Sequences. An extensive AC-rich specific sequence has been found in three different protamine gene containing clones isolated from a trout *Eco*RI Charon 4A library. This region is located in a similar position in all three clones, approximately 1 kilobase downstream from the protamine gene (Figure 1A). The protamine gene regions for TP17 and TP15 have been described previously (Aiken et al., 1983); TP103 is identical with TP15 in the protamine gene coding region and contains only three nucleotide changes within the region of 800 nucleotides sequenced.

Sequence analysis of the three clones (Figure 1B) indicates 56–60% of the $(AC)_n$-rich region consists of AC dinucleotides, but the sequence itself is specific and not entirely an alternating AC polymer. Other alternating purine–pyrimidine combinations are also very frequent in this region, with the result that a total of 86–88% of the sequence consists of alternating purine–pyrimidine dinucleotides (Figure 1C). Though considerable sequence homology is present, the length of the $(AC)_n$-rich regions is exceedingly variable. An $(AC)_n$-rich sequence of 57 base pairs is present in TP103; the region is

```
200                 220                 240                 260                 280
*                   *                   *                   *                   *
TTATTCTACTGTGTCCATTATCCATCCTGTTCAAAAGGTAGGTGCTTCAGCCTAGCTCAGTGCCTTCGGTGGTGCGGGGCGAACCAGCCAAAAAATAGGA

300                 320                 340                 360                 380
*                   *                   *                   *                   *
GCATTGCRCCGTGACTGGCGCAATGCGCTAAAAGGGTGGTCACACCAAAAATGTATTTGATGTAGATTTTTCTTCGGTTTACTCGCTTTGCATCTTGTAA

400                 420                 440                 460                 480
*                   *                   *                   *                   *
TTGATTAAATGTAATTTATTAACATGTCTATTTTTGAAAGCATTCTTACTTTACAGCATTTTTTCACACCTGCCTAAGACTTTTGCACAGTACTGTATGT

500                 520                 540                 560                 580
*                   *                   *                   *                   *
CCAGCATCCAGCATTCATTGTGTCCAGATGTGGATGGTGGTCATAAACCTTCCATCTCCATGAGGAAATAATAACAAGGTGGGAGGAAACGTGACGCCGT

600                 620                 640                 660                 680
*                   *                   *                   *                   *
CCTGGGAGGAGCTGCAAACCACTCTGTGACTGGACTGGTGAAATGCCACGGTGTCCATTACAATGTCAACGGTTGGCTGATTTCGCCTCACTGCAACCCT

700                 720
*                   *
TTCCTCACCTGGCTGCAACCCTTCCAGAGAGGTCATCCA
```

FIGURE 2: Nucleotide sequence 3′ of the $(AC)_n$-rich regions in TP17. The numbering begins at base 198, immediately following the $(AC)_n$-rich sequence presented in Figure 1B. A 17 base pair alternating purine–pyrimidine tract is underlined, with the interruptions in the alternating sequence being overlined.

129 nucleotides in length in TP15, while an extensive 195 base pair $(AC)_n$-rich sequence is found in TP17. Each $(AC)_n$-rich region in the three clones contains perfectly conserved 46 base pair repeats. Only one of these sequences is present in TP103, while TP15 contains two such repeats and TP17 has three. A schematic representation of the three AC-rich regions and their location relative to the protamine gene is presented in Figure 1A.

These sequences were searched against the GenBank data base for homologous sequences. The identity scores for both the AC and TG sequences ranged from 59% to 20%, and the sequences are arranged in descending order, as shown in Table I. Homologous AC and TG sequences were identified in the mammal, primate, and viral data bases. The TG sequences of the opposite strand in TP17 were also compared with TG sequences in the GenBank by the same technique, with the result that one additional homologous TG sequence was identified in the plant data base. As shown in Table I, the TP17 repeat sequences can be divided into three parts. The first is a relatively short 10 base pair (bp) AC or TG repeat, the second (as underlined) is a 46-bp repeat, and the third is a short spacer region of 22 bp. On this basis the homologous sequences can be grouped. AC sequences 2–4 and TG sequences 2–6 possessed significant homology, at least 75% over the entire TP17 repeat sequence. It is also clear that the homology that the majority of the other sequences showed was confined to either the 46-bp repeat and/or the 22-bp spacer region.

The region surrounding the $(AC)_n$-rich repeat in TP17 was also sequenced, and this led to the identification of several additional alternating purine–pyrimidine sequences downstream of the $(AC)_n$-rich region. Our criteria for identifying such sequences are five (or more) uninterrupted alternating purine–pyrimidines or eight (or more) with a single interruption (Miller et al., 1983). Though several regions meet these criteria, most are small (less than 13 nucleotides in length). There is, however, a more extensive alternating purine–pyrimidine tract, containing 17 nucleotides with only 2 interruptions present, 284 nucleotides downstream from the end of the $(AC)_n$-rich region (Figure 2).

Plasmid TP17, which was constructed by inserting a 3.6-kilobase *Bam*HI restriction fragment (containing both the protamine gene and the 195 base pair AC-rich region) into the *Bam*HI site of pBR322, was further analyzed by radioimmunoassay, immunoelectron microscopy, and S1 nuclease digestion. We have sequenced the protamine gene and its flanking regions (800 base pairs) as well as 800 nucleotides flanking the *Kpn*I site. Northern blots of poly(A+) and poly(A−) RNAs from both liver and testes indicate the only detectable RNA-hybridizing region in the plasmid is the protamine gene (data not shown).

Plasmid TP17 Binds Anti-Z DNA IgG. Subclone TP17 DNA was examined for its ability to compete with the binding of a polyclonal IgG preparation of anti-Z DNA IgG to left-handed [^{32}P]-labeled poly[d(Gm^{5}C)]. Two different assay conditions were tested. The high-salt assay was carried out in 4.0 M NaCl, 40 mM Tris-HCl (pH 7.2), and 4.0 mM EDTA at 54 °C while the low-salt assay was performed in 0.12 M NaCl, 40 mM Tris-HCl (pH 7.2), and 4 mM $MgCl_2$ at 37 °C. The results from the competitive radioimmunoassays are shown in Figure 3.

Superhelical (form I) and linear (form III) TP17 DNAs were tested as competitors, along with form I pBR322. Under both conditions, within the sensitivity of the assay, the superhelical form of TP17 competed effectively. In contrast, neither the linear form of TP17 nor the superhelical form of pBR322 inhibited the interaction of the antibody with poly[d(Gm^{5}C)] irrespective of the salt conditions. Therefore, effective competition for the anti-Z DNA IgG is dependent upon the presence of the trout protamine DNA insert and upon the torsional stress of supercoiling.

A comparison between the two assay conditions demonstrated that more TP17 DNA was required for inhibition in the low-salt reactions compared to the high-salt reactions. However, in the low-salt assay, the homologous competition curves with poly[d(Gm^{5}C)] and with PM2 DNA, a covalently closed circular genome shown to contain left-handed regions (Stockton et al., 1983), were also shifted to higher DNA concentrations. Although almost 300 times as much TP17 as poly[d(Gm^{5}C)] was required to cause 50% inhibition of binding of labeled poly[d(Gm^{5}C)], it should be noted that the 195 base pair $(AC)_n$-rich region only comprises 2.75% or $^1/_{36}$th of the total TP17 plasmid.

There is evidence to suggest that not all of the $(AC)_n$-rich repeat in TP17 is in the left-handed conformation at the natural superhelical density since TP103, which contains only one $(AC)_n$-rich repeating unit, also competed for the binding of anti-Z DNA IgG under high-salt conditions (data not presented). Although its plasmid did not compete as effectively at TP17, the difference in antibody binding was small when compared to the 3-fold difference in the size of the $(AC)_n$-rich repeat.

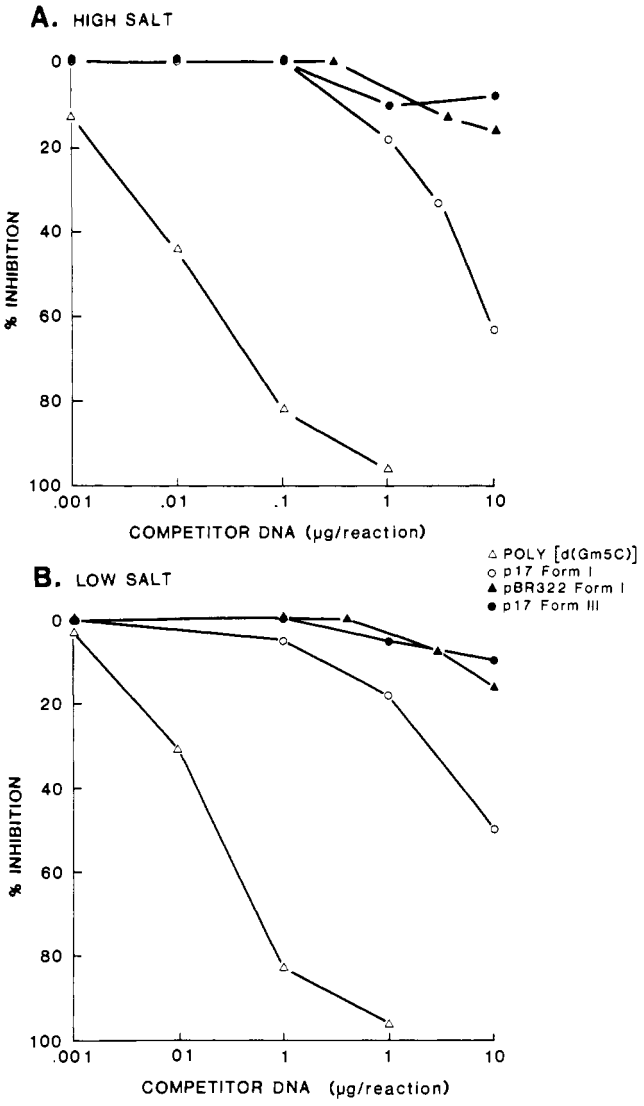

FIGURE 3: Results of a radioimmunoassay comparison between poly[d(Gm^{5}C)], pBR322 (form I), TP17 (form I), and TP17 (form III). Formation of the antibody–DNA complex was monitored by competition between unlabeled plasmid DNA and ^{32}P-labeled poly-[d(Gm^{5}C)] for Anti-Z IgG in either high salt (A) or low salt (B) as described under Experimental Procedures.

In later work using a two-dimensional gel technique (Wang et al., 1982) to separate topoisomers of pRSA, a construct in which two tandem 88-bp AC-rich regions of TP17 are inserted with *Bam*HI linkers into the *Bam*HI site of the small plasmid pUC9, it was calculated that 30 bp of the insert underwent the B to Z transition. This represents ca. one-third of a single $(AC)_n$ repeat, and there are three in TP17. Therefore, only ca. one-ninth of the total AC-rich region might be able to undergo the transition. The fact that 300 times as much TP17 as poly[d(Gm^{5}C)] is required to cause 50% inhibition of Z–antibody binding is consistent with only $^1/_9$th of the AC-rich region, which itself represents only $^1/_{36}$th of the total TP17 plasmid, being in the Z conformation ($^1/_9 \times {}^1/_{36} = {}^1/_{324}$).

There Is a Strong Correlation between Anti-Z DNA Antibody Binding Regions and Alternating Purine–Pyrimidine-Rich Sequences in TP17. The location of anti-Z DNA IgG binding to TP17 was investigated by immunoelectron microscopy. Plasmids containing the 3.6-kilobase *Bam*HI insert and either one or two pBR322 molecules were incubated with various anti-Z IgG concentrations in reactions containing either high or low monovalent salt prior to the addition of a ferritin-conjugated second antibody. Samples were subsequently fixed, dialyzed, and linearized by restriction endonuclease cleavage with *Kpn*I, which cleaves the plasmid 10 base pairs from the beginning of the $(AC)_n$-rich repeat. pBR322 molecules prepared in an identical manner and cleaved with the restriction endonuclease *Bam*HI show up to three anti-Z IgG–ferritin complexes. Four anti-Z DNA sites have been previously mapped in pBR322 at 1451 (Nordheim et al., 1982), 1410 ± 100, 960 ± 100, and 230 ± 100 base pairs (DiCapua et al., 1983). These sites in pBR322 were used to verify and orient the antibody binding region in the *Kpn*I-cleaved TP17 and TP17a (Figures 4 and 5). Twenty-eight DNA molecules were observed to bind a total of 72 antibody molecules; 29% of these antibodies bound within 400 base pairs of the cleaved ends of the TP17. The binding of 1–2 anti-Z IgG–ferritin complexes near the *Kpn*I site was present on 57% of the DNA molecules, in a region corresponding to the $(AC)_n$-rich sequence. An additional binding site, to which 7% of the antibody bound, was noted approximately 500 nucleotides from the $(AC)_n$-rich end, which correlates well with an S1-sensitive site (see next section). Sequence analysis of this region of TP17 indicates the presence of an alternating purine–pyrimidine segment 17 bases long (TGCACAGTACT-GTATGT) with two interruptions 481 bases from the start of the $(AC)_n$-rich region (see Figure 2). It should be noted that these alternating purine–pyrimidine tracts downstream from the protamine gene are longer than any left-handed sequences that have been reported to exist in pBR322. Sequence analysis of the protamine gene region of the insert does not reveal any alternating purine–pyrimidine sequences longer than six nucleotides.

S1-Sensitive Sites Are Adjacent to the $(AC)_n$-Rich Sequence. Single-stranded regions, sensitive to S1 nuclease, have been found to occur at the junction between left- and right-handed DNA domains in plasmids containing alternating GC (Singleton et al., 1982) as well as AC inserts (Singleton et al., 1984). The single strand specific S1 nuclease was used to demonstrate the presence of single-stranded regions adjacent to the $(AC)_n$-rich region in TP17.

TP17 was digested with varying concentrations of S1 nuclease and then cleaved with the restriction endonuclease *Msp*I. Treatment with S1 nuclease yields two additional bands not present in the *Msp*I digestion (Figure 6B). As only one *Msp*I restriction fragment is larger than the S1 bands, these bands, a diffuse band at 1.1–1.25 kilobases and a sharp but faint 1.6-kilobase band, must be derived from the 2.4-kilobase restriction fragment. This 2.4-kilobase fragment contains part of the protamine gene and the entire $(AC)_n$-rich region (Figure 6A).

The distances from the *Msp*I site located within the protamine gene (Figure 1) to the beginning and to the end of the $(AC)_n$-rich region are 1.1 and 1.25 kilobases (kb), respectively. Distances from the start and end of the $(AC)_n$-rich sequence downstream (in relation to the protamine gene) to the next *Msp*I site are similar, 1.1–1.3 kb. Thus, the S1 digestion bands of 1.1–1.25 kb correspond almost precisely with the bands predicted from the restriction endonuclease and DNA sequence data.

To confirm the presence of the $(AC)_n$-rich sequence within the 1.1–1.25-kb S1 fragments, the gel in Figure 6B was transferred to nitrocellulose and probed with an *Rsa*I fragment isolated from the $(AC)_n$-rich sequence of TP17 (positions −10 to +78, Figure 1B). The results of the autoradiography are presented in Figure 6C. Two hybridizing bands are evident, a 2.4-kb band, which corresponds to the intact *Msp*I fragment, as well as a heterogeneous band of 1.1–1.25 kb. These diffuse

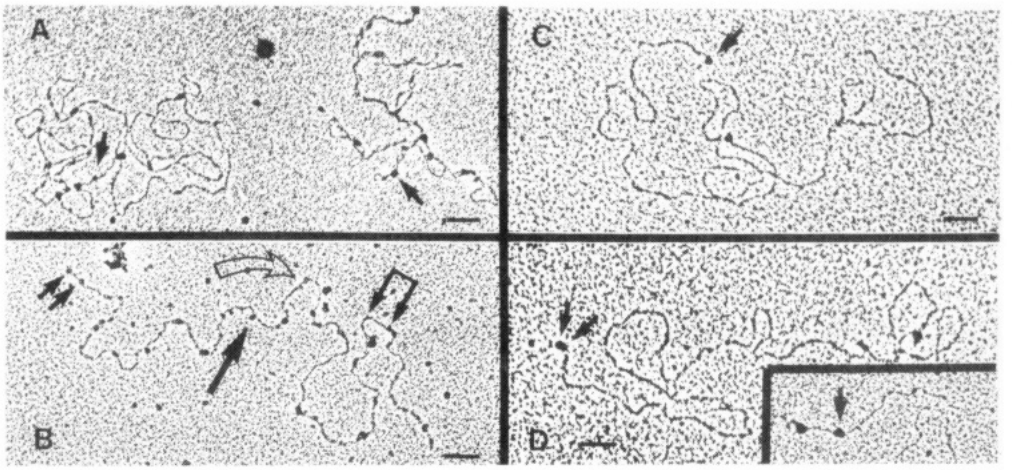

FIGURE 4: Electron micrographs: (A) cc form of TP17a (containing two pBR322 molecules) prepared under high-salt conditions at an antibody:TP17a ratio of 220:1. Multiple anti-Z IgG–ferritin complexes are associated with these molecules (arrows) (bar = 0.1 μm) (B) TP17 prepared under high-salt conditions at an antibody:TP17 ratio of 380:1, cleaved with *Kpn*I after fixation. Two complexes are present within the $(AC)_n$-rich region (two small arrows) while that portion of the molecule containing the protamine gene (brackets) shows no binding. Within the pBR322 component of the molecule, the anti-Z DNA antibody binding site at position 960 ± 100 (DiCapua et al., 1983) is indicated by a large solid arrow while a large open arrow refers to the region determined by Nordheim et al. (1982) at position 1451 and by DiCapua et al. (1983) at position 1410 ± 100. (bar = 0.1 μm). (C and D) Two examples of TP17 prepared under low-salt conditions at an antibody:TP17 ratio of 95:1 with either one (C) or two (D) anti-Z IgG–ferritin complexes (arrows) bound adjacent to the *Kpn*I site in the region of the $(AC)_n$-rich repeat (bars = 1.5 μm). The inset to (D) illustrates an additional complex (arrow) located 500 ± 100 base pairs from the end of the molecule.

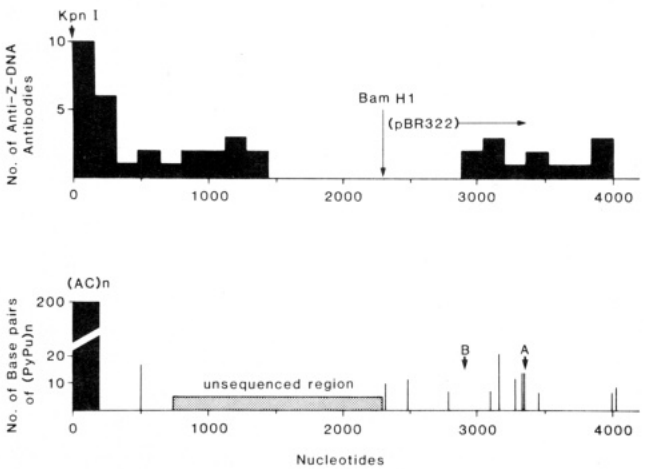

FIGURE 5: Correlation between antibody binding sites and alternating purine–pyrimidine regions in TP17 (map units 0.230–0.730). (Top) Histogram of fixed TP17–antibody complexes prepared under low-salt conditions and cleaved with *Kpn*I. Antibody binding sites were mapped from the *Kpn*I end, and the orientation was determined by a high degree of binding in the $(AC)_n$ region or in alternating purine–pyrimidine-rich regions in pBR322. Only complexes with a minimum of two and a maximum of six bound antibodies were used for the histogram. (Bottom) Length (vertical axis) and distribution of alternating purine–pyrimidine tracks within the map units 0.230–0.730. Only $(RY)_n$ sequences seven nucleotides or greater in length or ten nucleotides or greater with one interruption are plotted. Due to its size, the 195 base pair $(AC)_n$ region is displayed as a bar. The Z DNA site in pBR322 at nucleotide position 1451 (Nordheim et al., 1982) and 960 (Dicapua et al., 1983) are indicated by sites A and B, respectively.

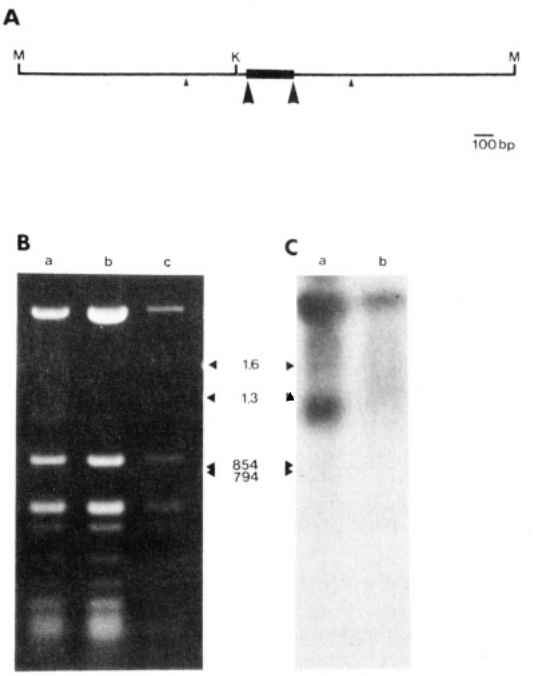

FIGURE 6: S1 nuclease studies (A) Schematic representation of the 2.4-kilobase *Msp*I fragment of TP17. The wide bar indicates the $(AC)_n$-rich sequence. The large arrows represent the S1 cut sites at the borders of the $(AC)_n$-rich sequence, and the small arrows indicate the S1 nuclease region of the protamine gene is near the left *Msp*I site. M = *Msp*I, K = *Kpn*I. (B) TP17 digested with varying amounts of S1 nuclease and 1 unit/μg *Msp*I, electrophoresed on 1.2% agarose, and stained with ethidium bromide. (a) 50 units of S1 nuclease per microgram of DNA followed by *Msp*I digestion. (b) 5 units of S1 nuclease per microgram of DNA followed by *Msp*I digestion. (c) *Msp*I digestion followed by 50 units per microgram S1 nuclease. Marker sizes are given in base pairs. (C) Hybridization of S1 nuclease treated DNA to the $(AC)_n$ probe (positions −12 to +78, Figure 1B). (a) 5 units of S1 nuclease per microgram of DNA followed by 1 unit per microgram *Msp*I. (b) *Msp*I digestion followed by digestion with 50 units of S1 nuclease.

bands correspond to the S1 bands noted in the ethidium bromide stained gel, thus confirming the presence of the $(AC)_n$-rich sequence within these fragments digested with S1.

As previously noted, there is a larger, less intense S1 band also evident (Figure 6C) that results from cleavage at an S1-sensitive site present 1.6 kb away from either end of the 2.4-kb *Msp*I fragment. Interestingly, an S1-sensitive site present 1.6 kb downstream from the *Msp*I site (located within the protamine gene) is in almost the precise location of the 17 base pair alternating purine–pyrimidine sequence 481 base pairs downstream from the start of the $(AC)_n$-rich sequence detected by immunoelectron microscopy (Figure 2).

Thus, the S1 data indicate the presence of two major S1-sensitive sites located in close proximity to the $(AC)_n$-rich sequence. These sites are present under low-salt conditions

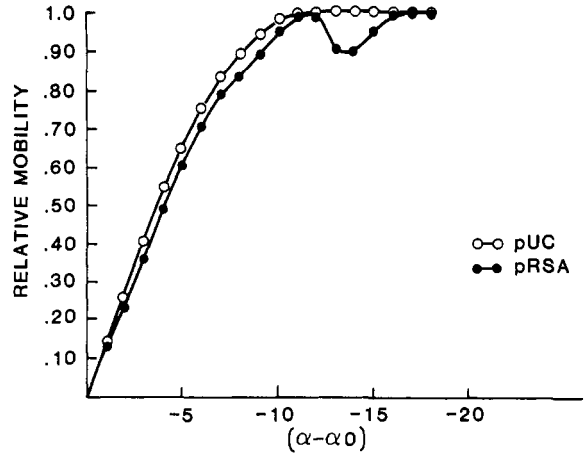

FIGURE 7: Electrophoretic mobility of form I topoisomers of pUC9 and pRSA. Individual topoisomers were scored for their mobility of the first dimension of two-dimensional gels relative to the nicked circular plasmid DNA. Data points are the average of *five* separate determinations for pRSA and *three* for pUC9. Plasmid pRSA was constructed by subcloning an 88-bp *KpnI–RsaI* restriction fragment containing the $(AC)_n$-rich region from the protamine gene containing plasmid TP17 (Aiken et al., 1983) into the *Bam*HI site of pUC9 (Viera & Messing, 1982) after attaching *Bam*HI linkers to the *RsaI* blunt ends. Subsequent analysis showed that RSA, in fact, contained two tandem 88-bp repeats.

(120 mM NaCl) and are dependent upon the torsional stress of supercoiling since S1 nuclease digestion following restriction endonuclease digestion does not give the two additional bands.

Two-Dimensional Gel Electrophoretic Analysis Indicates a B to Z Transition within the $(AC)_n$-Rich Region at Physiological Superhelical Density. To confirm the ability of at least part of the $(AC)_n$-rich region to undergo the B to Z transition, an *RsaI* fragment containing 88 bp of the AC-rich region from TP17 (see Figure 1) was subcloned into the very small 2700-bp plasmid pUC9, and the topological properties of the resultant plasmids (pRSA) were examined by two-dimensional electrophoretic analysis (Haniford & Pulleyblank, 1983a,b; Wang et al., 1982). A summary of the results obtained under a variety of electrophoretic conditions is shown in Figure 7. The control plasmid, pUC9, demonstrated continuously increased electrophoretic mobility with increasing superhelical density, while pRSA demonstrated discontinuous migration commencing at topoisomer 13. This topoisomer migrated in the first dimension with topoisomer 9; this decrease in migration was equivalent to a net loss of four superhelical turns. Electrophoretic migration in the first dimension remained the same for topoisomer 14 and then increased again with increasing superhelical density. These results are consistent with a continuous B to Z transition of approximately 30 base pairs within the $(AC)_n$-rich region, commencing at a superhelical density of −0.045.

These data therefore confirm the results obtained by S1 nuclease digestion and binding of the anti-Z DNA antibody. Further, they demonstrate that only part of the $(AC)_n$-rich region is maintained in the left-handed conformation at physiological superhelical density, in support of the results obtained by radioimmunoassay.

Discussion

The variation in the length of the three $(AC)_n$-rich regions in the three clones (Figure 1) was quite unexpected, considering the high level of homology exhibited by the protamine gene region in these clones. The three clones code for identical proteins and collectively show only 17 nucleotide changes within the 800 base pairs sequenced in the protamine gene region. Comparison of the sequence flanking the $(AC)_n$-rich region indicates very few differences between the three clones (data not presented). Thus the variability in this region seems to be restricted to the $(AC)_n$-rich sequence itself. It is interesting to note that this repeat structure usually occurs singly (Table I). In the case of TP17 and cytomegalovirus (CMV) Colburn DNA this repeat is reiterated 3 times whereas in the case of TP15 and fetal $^{G}\gamma$ and $^{A}\gamma$ globin the repeat is reiterated twice (Table I). Since these appear to be unique cases, it would support the view that for the function of this sequence only one unit may be required. This does not exclude the possibility that there may be a cooperative (enhanced) effect between tandemly joined units.

It would appear, therefore, that the $(AC)_n$-rich region has evolved at a faster rate than the protamine gene region. The large degree of homology shared among the three clones in the $(AC)_n$-rich region would argue against a random insertional event producing the variation. Recombination would appear to be the most likely mechanism, since displaced synapsis at meiosis and unequal crossing-over of the 46 base pair repeat plus the adjacent 22 base pair "spacer" sequence could account for the tandem repeats present in the region. Interestingly, a number of authors have suggested $(AC)_n$-rich sequences to be recombinational "hotspots" (Nordheim & Rich, 1983; Miesfeld et al., 1981; Slightom et al., 1980; Shen & Smithies, 1982). As the sequence variation of the $(AC)_n$ region is limited to the $(AC)_n$-rich sequence itself, our data would support such a contention.

Radioimmunoassay experiments indicate that, as a supercoiled plasmid, TP17 has the ability to assume a Z DNA conformation under both low- and high-salt conditions, and S1 nuclease data indicate the presence of S1-sensitive sites in and around the $(AC)_n$-rich sequence. Electron microscopic visualization of antibody–TP17 complexes demonstrates multiple antibody binding sites in the $(AC)_n$-rich sequence. (Indeed, it is likely that the number of molecules displaying antibody binding around the *KpnI* region is underrepresented in electron microscope preparations, since hindrance of the access of the restriction endonuclease to heavily antibody bound regions is likely to inhibit endonuclease digestion.) Two-dimensional electrophoretic analysis of a mixture of topoisomers of the construct pRSA [the very small 2700-bp plasmid pUC9 containing an 88-bp $(AC)_n$ insert from TP17] showed a discontinuity (Figure 7) in the mobilities of the topoisomers in the first dimension at topoisomer 13 [corresponding to a B to Z transition of approximately 30 bp or one-thid of the 88-bp $(AC)_n$ insert]. This divergence between the mobilities of the topoisomers of pUC9 and pRSA is characteristic for a B to Z conformational transition in the $(AC)_n$ insert region similar as shown for plasmids containing $(GC)_n$ (Peck et al., 1982) and $(AC)_n(GT)_n$ inserts (Haniford & Pulleyblank, 1983a,b). Thus it can be concluded that this $(AC)_n$-rich sequence in TP17 is responsible for a significant proportion of Z DNA immunoreactivity evident at physiological conditions.

In vitro evidence indicates there is a discernible order in which alternating purine–pyrimidine sequences can undergo the B → Z transition, with $(GC)_n > (AC)_n \gg (AT)_n$ both in polymers (Jovin et al., 1983) and in plasmids (Miller et al., 1984). $(GC)_n$ repeats, unlike $(AC)_n$ repeats, are not ubiquitous in eukaryotic genomes (Hamada et al., 1982). It may, therefore, be more common for $(AC)_n$-rich sequences to be involved in possible regulation by conformational transitions in the DNA than $(GC)_n$ tracts. Our data, including the two-dimensional topoisomer analysis of pRSA, suggest that

Table I: Comparison of the TP17 Repeat Sequences with Homologous Sequences[a]

	5′	aligned nucleotide sequences	3′
AC Sequences[b]			
1. TP 17 (AC) [sense strand]	4	CACACACACACTACACACATAGCATGCACACACATGCATTCTGACGCCACACACACACGCACACACACTACGTACAGG	83
2. Rat Repetitive Sequence Cluster	194	--------T-*----------C---A---------A--CATAT--A-*-----T----A---T----*---AC---	267
3. Mouse Ig κ V-Region	1171	-C--------*--------C-*--CA--------CA--CA-AC--A-*----------A---------	1235
4. Hamster Vimentin	32	---C-------C-*--CA--------CA--CA-AC--A---------G-G----TT-A-*-----G----	101
5. CMV	806	-----T----A-*-TTT---CGTG-T----A-----------A---------	858
6. CMV	611	-C--------CA--CA-AC--A-*----------A---------AG----	659
7. CMV	335	--A----TGT-----CA--CA-AC--A-*----------A----	377
8. Human IFN-Gamma	1334	----A-*--CA-A---C--A-*----------A----------*--C---	1380
9. Mouse Plasmacytoma c-MYC (NIRAD)	1976	--C-C-C-CA-C--CA--------CA--CA-AC--A-*----------A-----	2028
10. Mouse T(15:12) Translocation Region:c-MYC	660	--C-C-C-CA-C--CA--------CA--CA-AC--A-*----------A-----	712
11. Mouse Ig V_H from PCH104	13	-A--CA----------TTAA----------A---------	55
12. Bovine Chymosin A	1210	----------CA-ATGTA-ATGG----TGT----------	1251
13. Bovine Chymosin B	1215	----------CA-ATGTA-ATG-----TGT----------	1257
14. Bovine Chymosin C	1174	----------CA-ATGTA-ATG-----TGT----------	1216
15. FBJ MOV	4193	--------A*--TGCA--T-------AA-------	4226
16. Mouse Ig V_H from PCH105	27	--AT----------CA-AC--A-*-T-------	59
17. Human Enkephalin	2499	----------A----------T-G--	2528
18. AGM Alu-Family	349	--CC---T-TA----------A------	377
19. Human Prothrombin	1526	--C--T---------------	1546
20. EBV LIR (IR1)	1453	--GG---------------	1471
21. EBV LIR	1454	--GG---------------	1472

	5′	aligned nucleotide sequences	3′
TG Sequences[c]			
1. TP 17 (TG) [opposite strand]	83	CCTGTACGTAGTGTGTGTGCGTGTGTGTGGCGTCAGAATGCATGTGTGTGCATGCTATGTGTGTAGTGTGTGTG	4
2. Human CRF	601	----T-C-*----------C-------T*--GT-T----------**----------*------A--	670
3. SSV	134	-------T----------T*--GT-TG--TG--------TG--*----------*----------	196
4. Mouse Ig V_H from M167 (Seg 2)	122	---------TA----------T*--GT-TG--TG--------TG--AG*-------*----------	186
5. Human Cardiac Actin	95	----A-T-C-C--------T----------T*--GT-TG--TG--------TG--*-G-------	159
6. Mouse Fragment L10	908	--------T-C---------T*--TT-TGCAT---------T-CA-*---AA--C-*-----A--	969
7. Human Fetal $^{G}_{A}\gamma$-Globin	3185	-C----T----------T*--GT-CGC--G-----T--TG--*-G----A-*--C------	3243
8. Human Fetal $^{G}_{A}\gamma$- and $^{A}_{A}\gamma$-Globin	8121	-C------T----------T--GT-TCA--G-----	8159
9. Human Fetal $^{G}_{G}\gamma$-Globin	1116	-C----T----------T*--GT-CGC--G-----T--TG--*-G----A-*--C------	1174
10. Human Fetal $^{A}_{A}\gamma$-Globin Allele B	1108	-C----T----------*-*-CGC--G--------TG--*-G---CA-C*------	1164
11. Rabbit Embryonic β3-Globin	1778	--------T----------T*-C-T-TG-A-*-A------T--A--	1822
12. Human δ-β Globin Intergenic Repeat	93	----CTC-TT-T--A-GA-T----------T--GT-TG--TG--------	144
13. Human Fetal $^{A}_{A}\gamma$-Globin, Allele A	1116	-C------T----------T--GT-TCA--G-----	1154
14. Human Fibroblast Actin	22	-G---GT--*---------T----------	51
15. Rat RT1-4	67	-G-C---G----C-----TT----GC---C-----	102
16. Cucumber MV	44	----GT--*---------TTA--TA-----T---	76
17. Rat RT1-?	69	-C---G----C-----TT----GC---C-----	102
18. Rat RT1-3	69	-C---G----C-----TT----GC---C-----	102
19. Rat Asp-, Gly-, Glu-tRNA Cluster	313	-C---G----C-----TT----GC---C-----	346
20. Rat RT1-1	69	-C---G----C-----TT----GC---C-----	102
21. FBJ MOV	811	----*-T-T---C-----T---------	837
22. Soybean Actin	6	--------T--------T-T-T-C--	31
23. Spleen FFV	610	----*-T-T---------T------	633

[a] The Tp17 repeat sequences were searched against the GenBank data base, and homologous sequences were identified and aligned by using the Beckman MicroGenie Make Search program. Bases that were identical are indicated by dashes (-) and those different by the altered base (C, A, T, G). Gaps (*) were introduced and individual bases deleted (↑) for optimal sequence alignment. Sequences (from top to bottom) are listed as a function of decreasing overall identity. [b] AC sequences: (1) TP17 AC repeat (sense strand); (2) rat repetitive sequence cluster, poly(RY) region on 1.3 kb; (3) mouse lg κ germ line V gene: κ2; (4) hamster vimentin gene: exons 3 and 4, and flanks; (5) cytomegalovirus Colburn DNA, cell–virus homology region; (6) cytomegalovirus Colburn DNA, cell–virus homology region; (7) cytomegalovirus Colburn DNA, cell–virus homology region; (8) human immune interferon (IFN-γ) gene and flanks; (9) mouse plasmacytoma rearranged c-myc gene (NIARD); (10) mouse T(15:12) translocation region: c-myc exon 1 (chromosome 15); (11) mouse lg germ line H-chain V region from PCH104 (segment 1); (12) bovine chymosin A (rennin) mRNA; (13) bovine chymosin B (rennin) mRNA; (14) bovine chymosin C (rennin) mRNA (partial); (15) FBJ murine osteosarcoma virus (proviral) complete genome; (16) mouse lg germ line H-chain V region from PCH105 (segment 2); (17) human enkephalin gene, intron C (3′ end) and 3′ flank; (18) African green monkey Alu family sequence 3′ to ori; (19) human prothrombin gene, partial (6 introns and 5 exons); (20) Epstein–Barr virus long internal reiteration (IR1); (21) Epstein–Barr virus large internal repeat (*Bam*HI-W fragment). [c] TG sequences: (1) TP17 TG repeat (opposite strand); (2) human corticotropin-releasing factor (CRF) gene; (3) simian sarcoma virus (proviral) complete genome; (4) mouse lg active H-chain V region from M167 (segment 2); (5) human cardiac muscle actin gene 3; (6) mouse DNA fragment L10; (7) human fetal $^{G}\gamma$ and $^{A}\gamma$ hemoglobin genes; (8) human fetal $^{G}\gamma$ and $^{A}\gamma$ hemoglobin genes; (9) human fetal γ-globin G gene; (10) human fetal γ-globin A gene, allele B; (11) rabbit embryonic β3-globin gene; (12) human δ–β globin intergenic repeat; (13) human fetal γ-globin A gene, allele A; (14) human actin gene from fibroblast; (15) rat Asp-tRNA, Gly-tRNA, and Glu-tRNA gene cluster, clone RT1-4; (16) cucumber mosaic virus RNA3 with RNA4, complete sequence; (17) rat Asp-tRNA, Gly-tRNA, and Glu-tRNA gene cluster, clone RT1-2; (18) rat Asp-tRNA, Gly-tRNA, and Glu-tRNA gene cluster, clone RT1-3; (19) rat Asp-tRNA, Gly-tRNA, and Glu-tRNA gene cluster; (20) rat Asp-tRNA, Gly-tRNA, and Glu-tRNA gene cluster, clone RT1-1; (21) FBJ murine osteosarcoma virus (proviral) complete genome; (22) soybean actin gene; (23) spleen focus-forming virus (friend), complete provirus.

the entire 195 base pair $(AC)_n$-rich sequence in form I TP17 plasmid may not be in the left-handed conformation.

As shown in Table I, the repeats described here are unique, although possessing significant homology when compared to other sequences described previously. The $(AC)_n$- or $(TG)_n$-rich sequences adjacent to the protamine genes are nonrepetitive, containing alternating purine–pyrimidine segments that are adjacent to, yet out of phase with, each other. It is possible that these out of alternation segments may assume the Z DNA conformation under different conditions so that not only may the presence or absence of Z conformation be controlled but also the proportion of the region that is the left-handed conformation may be controlled.

The proximity of the $(AC)_n$-rich sequence to the protamine gene [1 kilobase or, in vivo, approximately five nucleosomes, or close to one turn of a 30-nm chromatin solenoid (Thoma et al., 1979)] suggests that it might play a role in the transcriptional regulation of the gene. A complete B → Z transition for the 61 base pair $(AC)_n$ region of TP103 could produce a loss of 11 superhelical turns in the DNA. With TP17 the effect would be even greater, potentially producing a change of 37 superhelical turns. Such a change in DNA topology could (potentially) have an enormous effect on chromatin structure as well as on protein–DNA interactions. However, Southern transfers of the seven protamine gene containing phages (Aiken et al., 1983) probed with the $(AC)_n$-rich sequence indicate this region may not be adjacent to all protamine genes, at least in the 3′ regions (data not presented). However, only short regions of DNA 5′ (upstream) of the protamine gene are present in these clones, so the presence of 5′ $(AC)_n$ regions cannot be excluded. Further, since we were only probing with the $(AC)_n$-rich repeat fragment, the presence of other alternating purine–pyrimidine regions would not be detected by this method.

A second potential function of $(AC)_n$ regions, in vivo, could be in the induction and stabilization of chromatin condensation. A form of left-handed DNA, Z* DNA, that consists of an insoluble network of fibers as the result of specific aggregation of Z DNA regions has been identified (van de Sande & Jovin, 1982; van de Sande et al., 1982). It is possible, therefore, that the interaction of left-handed regions, in vivo, might be involved in chromatin condensation. Interestingly, protamine polypeptides have also been shown to stabilize left-handed DNA (Russel et al., 1983). During spermatogenesis in the trout, protamine entirely replaces the somatic histones to produce the highly condensed, transcriptionally and replicationally inert nucleoprotamine (Dixon, 1972). There is evidence indicating the displacement of histones by protamine is ordered, that is, some specific regions are inactivated before others (Levy-Wilson et al., 1980). One can speculate that a B → Z transition could be the signal that triggers the binding of protamine to the region or conversely that the presence of the protamine in the nucleus stabilizes potential left-handed regions resulting in the condensation of chromatin.

Recent studies have indicated that transcriptionally inactive condensed chromatin is not immunoreactive to Z DNA specific antibodies since neither the micronucleus of ciliated protozoans (Robert-Nicoud et al., 1984) nor rat sperm nuclei (Morgenegg et al., 1983) bound the Z DNA antibodies. Interaction of the antibody with these exceedingly compact nuclei, however, is likely to be severely restricted. Thus a correlation between the lack of Z DNA conformation and the condensation of chromatin has not been conclusively demonstrated.

We do not have evidence, at this time, that the $(AC)_n$-rich region actually attains a left-handed conformation in vivo. Our

in vitro data suggest that energy inherently present in the underwound plasmid is required for the B → Z transition. To enable the region to attain a Z conformation, in vivo, other cellular factors might be required. One possibility is cytosine methylation, which has been shown to stabilize the left-handed conformation (Behe & Felsenfeld, 1981). Other factors such as protein–DNA interactions and the higher order chromatin structure of the region could provide the means by which B → Z transitions are regulated in the eukaryotic genome. For example, discrete chromosomal loops have been documented in both mitotic and meiotic chromosomes (Paulson & Laemmli, 1977; Rattner et al., 1980, 1981). In meiosis these chromosomal loops form in conjunction with the establishment of a discrete protein element, the synaptonemal complex, and many of the loops show pronounced transcriptional activity. Thus one aspect of this unique chromosomal organization may be the establishment of fixed chromosomal domains, analogous to circular plasmids whose superhelicity may be controlled by B → Z transitions, which may be related to the regulation of stage-specific transcription.

ACKNOWLEDGMENTS

We gratefully acknowledge Dr. D. Zarling for his generous gift of the T4 antibody. We also thank Bernd Kalisch for preparing labeled poly[d(Gm^{5}C)], Dr. D. J. McKay for the use of his DNA sequence analysis programs, and Marnie Cudmore for assistance in the preparation of the manuscript.

SUPPLEMENTARY MATERIAL AVAILABLE

References for the computer analysis, AC sequences, and TG sequences (4 pages). Ordering information is given on any current masthead page.

REFERENCES

Aiken, J. M., McKenzie, D., Zhao, H.-Z., States, J. C., & Dixon, G. H. (1983) *Nucleic Acids Res. 11*, 4907–4922.

Arndt-Jovin, D. J., Robert-Nicoud, M., Zarling, D. A., Greider, C., Weimer, E., & Jovin, T. M. (1983) *Proc. Natl. Acad. Sci. U.S.A. 80*, 4344–4348.

Behe, M., & Felsenfeld, G. (1981) *Proc. Natl. Acad. Sci. U.S.A. 78*, 1619–1623.

DiCapua, E., Satsiak, A., Koller, Th., Brahms, S., Thomae, R., & Pohl, F. M. (1983) *EMBO J. 2*, 1531–1535.

Dixon, G. H. (1972) *Acta Endocrinol. (Copenhagen), Suppl. No. 168*, 130–154.

Gill, J. E., Mazrimas, J. A., & Bishop, C. C., Jr. (1974) *Biochim. Biophys. Acta 335*, 330–348.

Hamada, H., & Kakunaga, T. (1982) *Nature (London) 298*, 396–398.

Hamada, H., Petrino, M. G., & Kakunaga, T. (1982) *Proc. Natl. Acad. Sci. U.S.A. 79*, 6465–6469.

Haniford, D. B., & Pulleyblank, D. E. (1983a) *Nature (London) 302*, 632–634.

Haniford, D. B., & Pulleyblank, D. E. (1983b) *J. Biomol. Struct. Dyn. 1*, 593–609.

Jovin, T. M., van de Sande, J. H., Zarling, D. A., Arndt-Jovin, D. J., Eckstein, F., Fuldner, H. H., Greider, C., Grieger, I., Hamori, E., Kalish, B., McIntosh, L. P., & Robert-Nicoud, M. (1982) *Cold Spring Harbor Symp. Quant. Biol. 47*, 143–154.

Jovin, T. M., McIntosh, L. P., Arndt-Jovin, D. J., Zarling, D. A., Robert-Nicoud, M., van de Sande, J. H., Jorgenson, K. F., & Eckstein, F. (1983) *J. Biomol. Struct. Dyn. 1*, 21–57.

Lee, J. S., & Morgan, A. R. (1979) *Nucleic Acids Res. 5*, 2425–2434.

Levy-Wilson, B., Kuehl, L., & Dixon, G. H. (1980) *Nucleic Acids Res. 8*, 2859–2868.

Lipps, H. J., Nordheim, A., Lafer, E. M., Ammerman, D., Stollar, B. D., & Rich, A. (1983) *Cell (Cambridge, Mass.) 32*, 435–441.

Maniatis, T., Fritsch, E. F., & Sambrook, J. (1982) *Molecular Cloning*, Cold Spring Harbor Laboratory, Cold Spring Harbor, NY.

Maxam, A., & Gilbert, W. (1980) *Methods Enzymol. 65* 499–560.

Miesfeld, R., Krystal, M., & Arnheim, N. (1981) *Nucleic Acids Res. 9*, 5931–5937.

Miller, F., Jorgenson, K. F., Winkfein, R. J., van de Sande, J. H., Zarling, D. A., Stockton, J., & Rattner, J. B. (1983) *J. Biomol. Struct. Dyn. 1*, 611–620.

Morgenegg, G., Celio, M. R., Malfoy, B., Leng, M., & Kuenzle, C. C. (1983) *Nature (London) 303*, 540–543.

Nishioka, Y., & Leder, P. (1980) *J. Biol. Chem. 255*, 3691–3694.

Nordheim, A., & Rich, A. (1983) *Nature (London) 303*, 674–679.

Nordheim, A., Pardue, M. L., Lafer, E. M., Moller, A., Stollar, B. D., & Rich, A. (1981) *Nature (London) 294*, 417–422.

Nordheim, A., Lafer, E. M., Peck, L. J., Wang, J. C., Stollar, B. D., & Rich, A. (1982) *Cell (Cambridge, Mass.) 31*, 309–318.

Paulson, J. R., & Laemmli, U. K. (1977) *Cell (Cambridge, Mass.) 12*, 817–828.

Peck, L. J., Nordheim, A., Rich, A., & Wang, J. C. (1982) *Proc. Natl. Acad. Sci. U.S.A. 79*, 4560–4569.

Rattner, J. B., Goldsmith, M. R., & Hamkalo, B. A. (1980) *Chromosoma 79*, 215–224.

Rattner, J. B., Goldsmith, M. R., & Hamkalo, B. A. (1981) *Chromosoma 82*, 341–351.

Robert-Nicoud, M., Arndt-Jovin, D. J., Zarling, D. A., & Jovin, T. M. (1984) *EMBO J. 3*, 721–731.

Russel, W. C., Precious, B., Martin, S. R., & Bayley, P. M. (1983) *EMBO J. 2*, 1647–1653.

Saffar, J. D., & Lerman, M. I. (1983) *Mol. Cell. Biol. 3*, 960–964.

Shen, S.-H., & Smithies, O. (1982) *Nucleic Acids Res. 9*, 5931–5947.

Singleton, C. K., Klysik, J., Stirdivant, S. M., & Wells, R. D. (1982) *Nature (London) 299*, 312–316.

Singleton, C. K., Kilpatrick, M. W., & Wells, R. D. (1984) *J. Biol. Chem. 259*, 1963–1967.

Slightom, J. L., Blevchl, A. E., & Smithies, O. (1980) *Cell (Cambridge, Mass.) 21*, 627–638.

Stockton, J. F., Miller, F. D., Jorgenson, K. F., Zarling, D. A., Morgan, A. R., Rattner, J. B., & van de Sande, J. H. (1983) *EMBO J. 2*, 2123–2128.

Thoma, F., Koller, Th., & Klug, A. (1979) *J. Cell Biol. 83*, 403–427.

van de Sande, J. H., & Jovin, T. M. (1982) *EMBO J. 1*, 115–120.

van de Sande, J. H., McIntosh, L. P., & Jovin, T. M. (1982) *EMBO J. 1*, 777–782.

Viera, J., & Messing, J. (1982) *Gene 19*, 259–268.

Wang, J. C., Peck, L. J., & Bechener, K. (1982) *Cold Spring Harbor Symp. Quant. Biol. 47*, 85–91.

Zarling, D. A., Arndt-Jovin, D. J., Robert-Nicoud, M., McIntosh, L. P., Thomae, R., & Jovin, T. M. (1984) *J. Mol. Biol. 176*, 369–415.